Baku State University: Journal of Physics & Space Sciences, **2025**, v 2 (1), p. 58-69

journal homepage: http://bsuj.bsu.edu.az/en

Thermal stability and structural integrity in polystyrene composites with TIO_2 nanoparticles

Almara M. Rahimli*[1], Aybeniz S. Huseynova[2]

[1]Nano Research Laboratory, Baku State University, Baku, Azerbaijan
[2]Republic of Azerbaijan Ministry of Science and Education Institute of Physics, Baku, Azerbaijan

Received 17-Jan-2025; Accepted 12-Mar-2025
DOI: https://doi.org/10.30546/209501.101.2025.2.300.016

Abstract

The structural, thermal, and optical properties of TiO_2/Polystyrene (PS) nanocompositeswere investigated to understand the effects of incorporating rutile-phase TiO_2 nanoparticles. The nanocomposites were synthesized using a solution mixing method followed by hot pressing. Structural analysis, revealed that the crystallite size increased and strain decreased as TiO_2 content increased, indicating a structural evolution. SEM-EDX analysis confirmed uniform distribution of TiO_2 within the PS matrix. Thermal analysis via DSC showed a significant increase in the melting temperature (Tm), rising by up to 41°C, reflecting enhanced thermal stability due to restricted polymer chain mobility. TGA results demonstrated improved thermal stability, with a significant shift in decomposition temperatures from 450°C for pure PS to 480°C for PS/10%TiO_2, highlighting the positive effect of TiO_2 nanoparticles in enhancing the heat resistance of the nanocomposites.

Keywords: Activation energy; Interfacial polarization; Thermal behavior; Mass loss patterns
PACS: 01.55.+b; 61.46.+w; 65.40.-b; 65.80.-g

1. Introduction

Polymer composite materials have garnered significant attention for their ability to combine the advantageous properties of polymers and nanofillers, resulting in materials with enhanced functionalities [1-3]. Among thermoplastics, polystyrene

---

* *Corresponding author*. Tel.: (+994) 50 355 52 05.
e-mail: rahimli.almara@gmail.com; ORCID ID: 0009-0001-0652-3561.

(PS) is notable for its excellent mechanical properties, thermal stability, and processability, making it suitable for a variety of industrial and technological applications, including packaging, insulation, and electronics [2]. To meet the growing demand for advanced materials with tailored properties, the integration of nanofillers such as titanium dioxide (TiO_2) has become a key area of research [4]. Rutile-phase TiO_2, known for its high refractive index, ultraviolet (UV) absorption, and photocatalytic activity, is especially attractive due to its exceptional optical and thermal characteristics [5].

Despite the growing interest in TiO_2-based polymer composites, several studies have highlighted the challenges in achieving optimal dispersion and reinforcing effects. For example, Bendaoued et al. [7] incorporated TiO_2 nanoparticles into polypropylene composites via the sol–gel method, reporting improvements in thermal stability and rheological properties. Similarly, Alsulami and Rajeh [8] examined polyaniline/polymethyl methacrylate composites doped with TiO_2, revealing enhanced thermal stability but did not address the role of TiO_2 in altering the structural characteristics of the polymer matrix.

Further investigations by KudililEsthappan et al. [9] and Bikiaris et al. [10] explored the incorporation of TiO_2 and silica nanoparticles into polypropylene and isotactic polypropylene, respectively, but the effect of TiO_2 concentration on crystallinity and the interactions between TiO_2 and PS remained insufficiently explored. The current literature suggests a lack of understanding regarding the precise role of TiO_2 concentration in modulating the structural, thermal, and optical properties of polymer composites.

This study addresses these gaps by focusing on the structural, thermal, and optical properties of rutile-phase TiO_2/PS nanocomposites with varying nanoparticle concentrations (3%, 5%, and 10%).

2. Materials and Methods

All chemicals were used as received without undergoing purification. Polystyrene (PS) (CAS number 9002-86-2)was characterized by a density of 1.04 g/cm^3, a melting temperature range of 150–220°C, a flash point of 625°C, an ignition temperature of 500°C, and an auto-ignition temperature exceeding 1100°C. Tetrahydrofuran (THF) with product code 143537 was also used as received. Titanium oxide nanoparticles with a particle size ranging from 30 to 50 nm were procured from Sky Spring Nanomaterials, Inc.

The polymer nanocomposite materials were synthesized via combination of two methods, namely solution-mixing and hot-pressing process. Initially, polystyrene was dissolved in tetrahydrofuran (THF), its organic solvent. Titanium oxide nanoparticles, with varying concentrations of 1%, 5%, and 10%, were accurately weighed and added to the PS-THF solution. The mixture was stirred vigorously for 2 hours to ensure thorough dispersion of TiO2 nanoparticles within the PS-THF solution. Subsequently, the resulting mixture was poured into a Petri dish and left to air-dry for 24 hours. To completely remove the solvent from the polymeric matrix, the nanocomposites were further dried in a vacuum oven at room temperature for 1 hour. Thin films of the nanocomposites were then prepared using the hot pressing method at 180°Cand 10 MPa. The films were cooled post-hot pressing by immersion in water.

TiO_2 concentrations of 3%, 5%, and 10% were selected based on preliminary trials. A 1% TiO_2 concentration had minimal impact on the properties, similar to the pure PS. At higher concentrations (15% and 20%), the polymer matrix could not accommodate the excessive nanoparticle content, leading to poor dispersion and structural degradation. The 10% TiO_2 concentration was optimal, showing significant improvements without structural compromise. Higher concentrations led to a percolation effect, where further increases in TiO_2 did not enhance, and could hinder the nanocomposite properties.

X-ray diffraction (XRD) analysis was performed using a Rigaku Mini Flex 600 XRD diffractometer at room temperature. Cu Kα radiation, operating at 15 mA and 30 kV was used for all experiments. The samples were scanned over a 2θ range of 10–90°.The average crystallite size (D) for the nanocomposites was calculated using Scherrer's formula:

$$D = \frac{K\lambda}{\beta cos\theta} \tag{1}$$

Here, D represents the grain size (or crystallite size) of the material, λ is X-Ray wavelength, θ is the diffraction angle, β is the full width at half maximum (FWHM) of the observed peak (in radians), and K is the shape factor, equal to 0.89 [11-14].

The surface morphology of the nanocomposites was examined using a scanning electron microscope (SEM; JEOL JSM-6610 LV), to analyze the dispersion and size of nanoscale TiO_2 nanoparticles in the polymer. The SEM scanning was performed at an accelerating voltage of 30 kV.

Differential scanning calorimetry (DSC) and thermogravimetric analysis (TGA) were conducted in the temperature range T=20-550°C using an STA3000 Synchronous Thermal Analyzer at a heating rate of 25°C/min. Ceramic (Ce) cuvettes were used during the experiment. The experiment was conducted in a nitrogen (N_2) atmosphere. Samples were heated from 20°C to 550°C at a rate of 20°C/min. Each sample weighed approximately 85-87 mg. This temperature range was chosen to capture the significant thermal transitions in polystyrene (PS) and its nanocomposites, offering insights into polymer matrix's stability near its degradation temperature.

3. Results and Discussions

The XRD patterns for polystyrene (PS) and PS-based nanocomposites with increasing TiO_2 concentrations (3%, 5%, and 10%) are given in Figure 1.Pure PS exhibits a broad peak around 20°, characteristic of its amorphous structure [1]. As TiO_2 content rises, distinct peaks emerge corresponding to the rutile phase of TiO_2, specifically at 17.86° (002), 20.02° (111), 20.64° (001), 27.4° (110), 36.1° (101), 39.2° (200), 41.2° (111), 44.0° (210), 56.6° (220), and 69.0° (301) [3-5]. These peaks become increasingly prominent with higher TiO_2 concentrations, indicating effective incorporation and enhanced crystallinity of the TiO_2 nanoparticles.

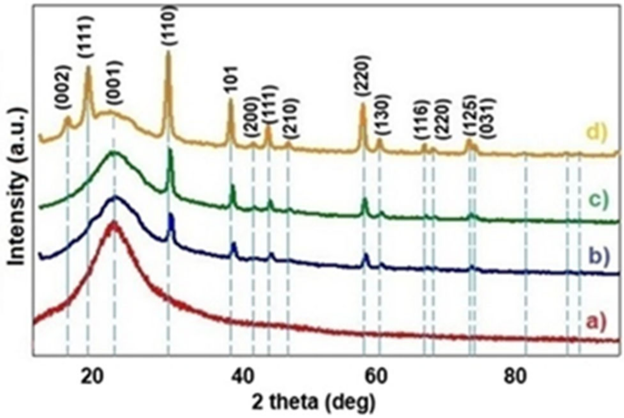

Fig. 1. XRD spectra for: a) Pure PS; b) PS/3%TiO_2; c) PS/5%TiO_2; d) PS/10%TiO_2basednano-composites

As the TiO_2 concentration increases, several trends emerge in the crystallite size, strain, and dislocation density. At lower TiO_2 concentrations (3% and 5%), the crystallite size is smaller, but increases as the TiO_2 content reaches 10%, suggesting that higher TiO_2 concentrations promote crystalline growth within the PS matrix, likely due to the nucleating effect of TiO_2 nanoparticles. The strain, which indicates internal stress, is highest in the 3%TiO_2 sample, reflecting greater distortions in the PS structure with a small amount of TiO_2. As TiO_2 concentration increases, strain decreases, which suggests that higher TiO_2 concentrations help stabilize the structure, likely by improving nanoparticle distribution and reducing local stress. Similarly, the dislocation density, a measure of crystal imperfections, follows a similar trend. It is highest in the 3% TiO_2 sample, suggesting greater structural defects, possibly due to poor nanoparticle dispersion. As TiO_2 concentration increases, the dislocation density decreases, indicating better nanoparticle dispersion and fewer defects at higher concentrations, leading to a more ordered structure. Our findings align with those of Gareso et al. [14].

The SEM image of pure PS (Fig. 3a) shows a smooth, featureless surface, typical of a homogeneous polymer. EDS analysis reveals carbon (C) at 92.71 wt% and oxygen (O) at 7.29 wt%, consistent with polystyrene's composition. This confirms the sample's purity.

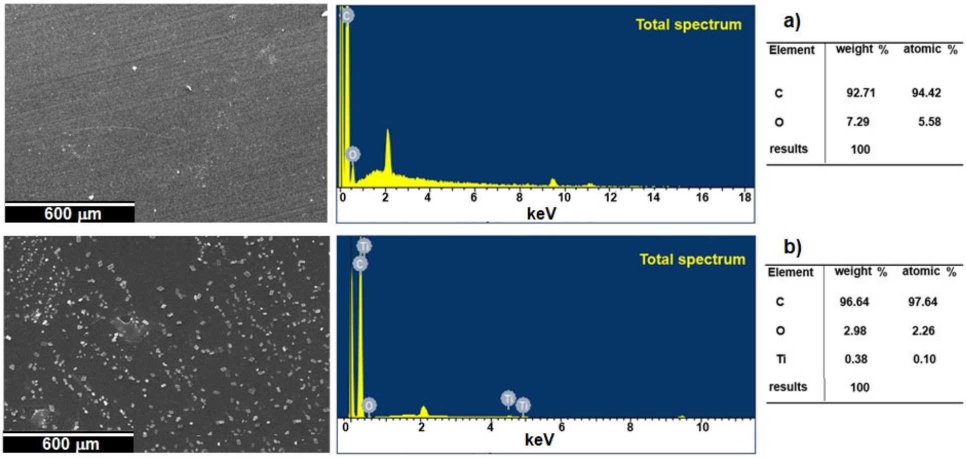

a)

Element	weight %	atomic %
C	92.71	94.42
O	7.29	5.58
results	100	

b)

Element	weight %	atomic %
C	96.64	97.64
O	2.98	2.26
Ti	0.38	0.10
results	100	

Fig. 2. SEM image and corresponding EDX spectra of PS (a), PS/TiO_2 (b) nanoparticles

In contrast, the TiO_2 nanoparticles (Fig. 2, b) exhibit a distinct particulate morphology, with particles dispersed over the surface. The granular appearance is characteristic of TiO_2, with well-defined particles contrasting against the smoother PS surface. EDS analysis confirms titanium (Ti) at 0.38%, alongside 2.98% oxygen, and a high carbon content of 96.64%, which may stem from the carbon coating or sample preparation process.

Figure 3 shows the surface morphology (a) and size distribution (b) of TiO_2 nanoparticles at x100,000 magnification, with sizes ranging from 32.6 nm to 68.5 nm.The nanoparticles are well-dispersed, with minimal aggregation, suggesting effective distribution within the PS matrix. The average particle size is50.4 nm, calculated based onmeasurements of individual nanoparticles. These measurements align with the reported TiO_2 size range of 30-50 nm, indicating effective dispersion within the PS matrix without significant agglomeration. The TiO_2 nanoparticles embedded in the polymer suggest a uniform distribution, beneficial for enhancing the composite's properties.

The histogram shows a narrow size distribution of the nanoparticles (Fig. 4b). This uniform distribution enhances interfacial interactions between the nanoparticles and the polymer matrix, influencing the nanocomposite's structural, thermal, and optical properties.

.

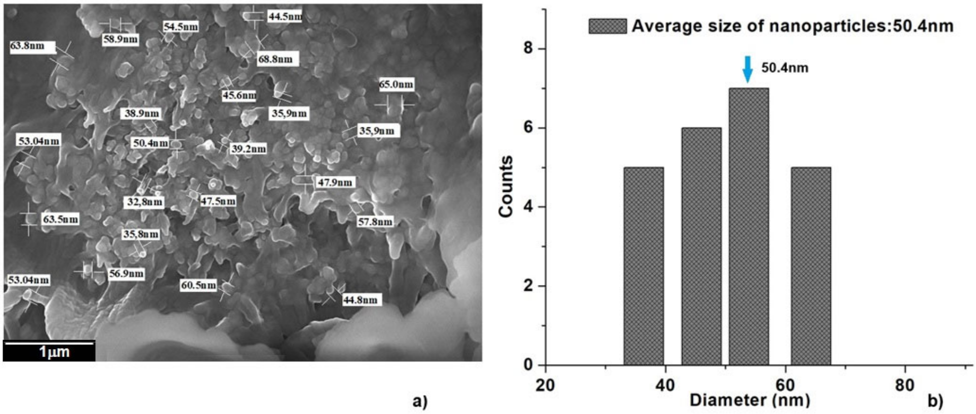

Fig. 3. SEM micrograph (a) and size distribution histogram (b) of PS/TiO_2 nanocomposite (average nanoparticle size: 50.4 nm)

The thermal behavior of pure PS and PS/TiO_2nanocomposites was analyzed using thermogravimetric analysis (Fig. 4). The decomposition patterns vary significantly with the addition of TiO_2 nanoparticles.

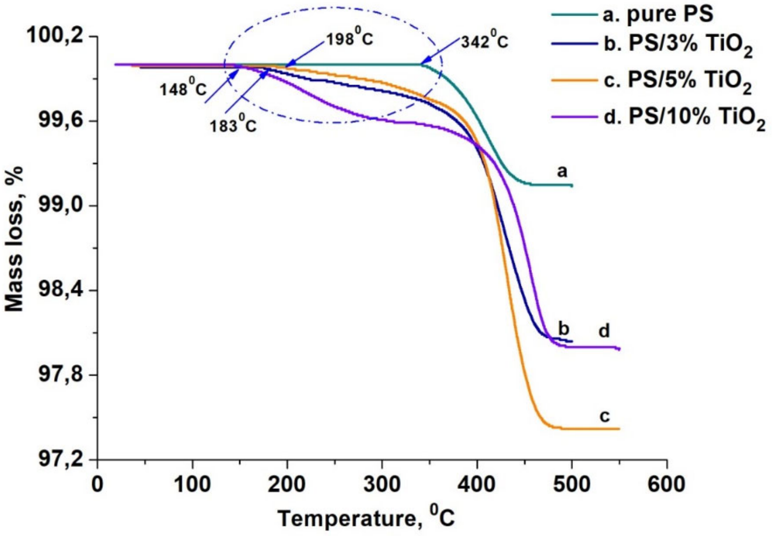

Fig. 4. TG curves for pure PS and PS/TiO_2nanocomposites done at 25°C min^{-1} heating rate under N2 atmosphere

Thermal stability indicators of PS and PS/TiO_2nanocomposites, calculated from the spectra,are summarized in Table 2.Pure PS shows an initial decomposition temperature of 342.14°C, while TiO_2 nanoparticles reduce this temperature to

176.17°C, 187.8°C, and 142.85°C for PS/3% TiO_2, PS/5% TiO_2, and PS/10%TiO_2, respectively (Table 2). This reduction is likely due to TiO_2 nanoparticles acting as catalytic sites, promoting polymer chain cleavage in the PS matrix. This process may involve mechanisms like free radical formation or localized chain scission near the nanoparticle interface [15, 16].

A slight decrease in decomposition temperature was observed at higher TiO_2 concentrations, particularly for PS/10%TiO_2, where the initial temperature dropped from to 142.85°C (PS/10%TiO_2) from 176.17°C (PS/3%TiO_2) and 187.8°C (PS/5%TiO_2) (Table 2). This suggests an optimal concentration beyond which the nanoparticles no longer effectively improvethermal resistance. This decrease may be due to specific interactions between the polymer and nanoparticles or the limitations of TiO_2 as a stabilizing agent at higher concentrations.Bikiaris et al. observed that some nanoparticles initially reduce the decomposition temperature but later improve thermal stability by forming protective barriers at elevated temperatures, a behavior also seen in our study [17].

At elevated temperatures, the intrinsic thermal stability of TiO_2 nanoparticles becomes dominant. These nanoparticles form protective barriers that inhibit heat transfer, slowing the degradation of the remaining polymer chains. This dual behavior- facilitating degradation at lower temperatures and stabilizing the material at higher temperatures -explains the unique thermal behavior of the nanocomposites.

The dual role of TiO_2 nanoparticles as both a degradation facilitator at low temperatures and a thermal stabilizer at high temperatures, has been previously reported. Montazer and Ali (2012) also note that TiO_2 acts as a stabilizing agent at elevated temperatures, forming protective layers that enhance the thermal stability of polymer nanocomposites under extreme conditions [18].

Additionally, the increased glass transition temperature (Tg) and melting temperature (Tm) observed in the DSC analysis suggest restricted polymer chain mobility due to strong interactions at the TiO_2-PS interface. These interactions enhance the thermal stability of the nanocomposites under thermal stress.

Figure 5 presents the DSC analysis, offering insights into the melting behavior of PS/TiO_2-based polymer nanocomposites.

The glass transition temperatures (Tg1, Tg2, Tg3) correspond to PS/3%TiO2, PS/5%TiO2, and PS/10%TiO2, respectively. The increase in Tg values with higher PS/TiO2 content indicates restricted polymer chain mobility, likely due to strong interfacial interactions between the polymer matrix and TiO2 nanoparticles. The curves also show endothermic transitions at higher temperatures, corresponding to melting or the onset of thermal degradation. These peaks represent the energy needed to overcome intermolecular forces and facilitate phase changes, providing key information on the thermal stability and phase behavior of the nanocomposites [17]. Notably, PS/10%TiO_2 shows a more prominent peak, suggesting enhanced thermal stability, likely due to the effective dispersion of TiO_2nanoparticles.

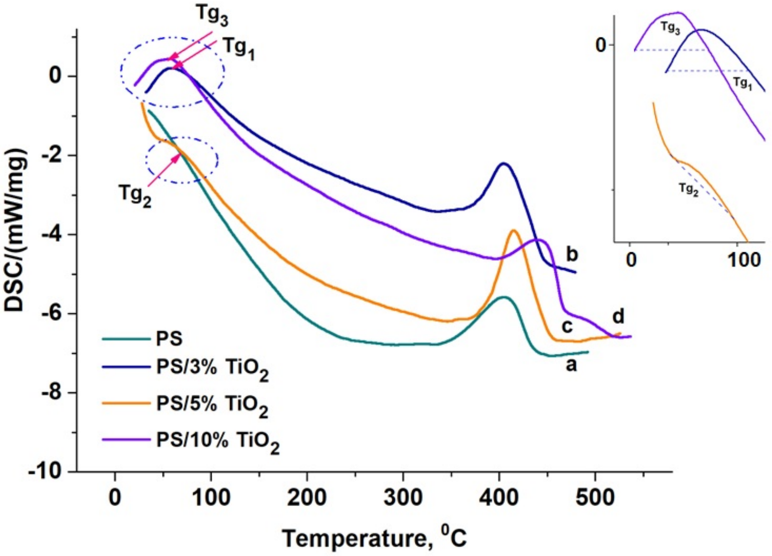

Fig. 5. DSC curves for pure PS and PS/TiO_2nanocomposites done at 25°C min^{-1} heating rate under N2 atmosphere

Furthermore, the interplay between TiO_2 concentration and processing conditions, such as hot-pressing variables, influences the crystalline-to-amorphous ratio. This suggests that tailored processing parameters can optimize the thermal and mechanical properties of PS/TiO_2nanocomposites for specific applications [19, 20].

For example, while higherTiO_2 loadings enhance rigidity and thermal stability, they may also affect processability due to increased thermal absorption and material stiffness. Therefore, achieving an optimal nanoparticle concentration is crucial for balancing these properties [21].

These findings highlight the potential of PS/TiO_2nanocomposites in applications requiring materials with enhanced dimensional stability under heat. The ability to tune their thermal and structural behavior through controlled nanoparticle loading and processing conditions makes them suitable for advanced industrial applications, such as UV shielding, thermal insulation, and high-temperature environments.

Figure 6 presents the Raman spectra highlighting the characteristic vibrational modes of pure PS and PS/TiO_2nanocomposites.As shown in the Figure 6, weak peaks at 405 cm^{-1} (C-C bending modes), 485 cm^{-1} (bending of C-H bonds), and 539 cm^{-1} (symmetric stretching modes of C-C or C-O bonds) in the spectrum of pure PS are absent in the spectra of PS/TiO_2nanocomposites. [24] The absence of these peaks suggests that the addition of TiO_2 affects the molecular vibrations within the PS matrix, potentially altering its structural integrity and interactions. In contrast, a peak observed at 447 cm^{-1} in the spectra of PS/TiO_2nanocomposites (Fig. 6, b-d), absent in the matrix (PS), appears more intensely in the spectrum of the PS/10%TiO_2nanocomposite.

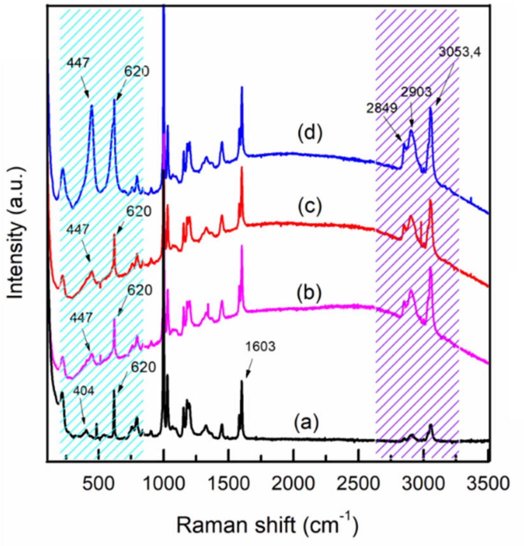

Fig. 6. Raman spectra for pure PS and PS/TiO_2nanocomposite at different concentrations of TiO_2: a) PS; b) PS/3% TiO_2; c) PS/5%TiO_2; d) PS/10% TiO_2

In the PS spectrum, the peak at 618 cm^{-1} may be related to the bending of carbon-carbon (C-C) or carbon-hydrogen (C-H) bonds in its molecular structure (Fig. 6, a). This peak may also reflect the vibrations of ester groups (-COO-), which are key components of PS. The intensification of this peak in the spectrum of the PS/10%TiO_2nanocomposite suggests that TiO_2 contributes to these vibrations, indicating a possible interaction between the TiO_2 nanoparticles and the PS matrix that enhances specific vibrational modes (Fig. 6, d).

The peaks at 1001 and 1032 cm^{-1} correspond to C-C stretching vibrations, indicative of the polymer backbone's structural integrity. Meanwhile, the peaks at 1155, 1181, and 1201 cm^{-1} correspond to in-plane C-H bending modes, revealing how the introduction of TiO_2 nanoparticles may influence the orientation and mobility of polymer chains within the matrix. The peak at 1450 cm^{-1} is associated with CH_2 bending vibrations (deformation modes), indicating changes in the conformation of polymer segments [22]. The peak at 1603 cm^{-1} relates to the stretching of C=C aromatic rings, which may suggest interactions with the aromatic components of the PS matrix.

Furthermore, the relatively intense and weaker peaks at 2903 and 3053 cm^{-1} mainly represent C-H stretching vibrations. This can also be attributedto as the vibrations of aliphatic groups (e.g., CH_3 or CH_2) in PS, which play a crucial role in the material’s physical properties.

Understanding these changes is crucial for optimizing the performance of the PS/TiO_2nanocomposites in potential applications, such as in coatings, electronics, or environmental remediation, where enhanced mechanical properties or photocatalytic activity are desired [24].

4. Conclusion

This study highlights the significant impact of rutile-phase TiO_2 nanoparticles on the structural, thermal, and optical properties of PS-based nanocomposites. XRD showed that increasing TiO_2 content led to larger crystallites and reduced strain, emphasizingthe structural evolution of the composites. SEM-EDX confirmed the uniform distributionof TiO_2 within the PS matrix. DSC analysis showed a significantincrease in the melting temperature (T_m) by up to 41°C, while TGA results indicated improvedthermal stability, with decomposition temperatures reaching 480°C compared to 450°C for pure PS. These findings highlightthe potential of TiO_2/PS nanocomposites for high-temperature applications, such as protective coatings and optoelectronic devices, and provide new insights into the optimization of polymer nanocomposites for industrial use.

References

[1] Rahimli, A., Huseynova, A., Musayeva, N., Alekperov, R., &Jafarov, M. Insights into dielectric and thermal properties of polystyrene-zinc oxide nanocomposites: A multifaceted characterization approach. Journal of Thermoplastic Composite Materials. 2024;0(0). doi:10.1177/08927057241274265

[2] Almara R, Huseynova A, Musayeva N. Comprehensive analysis OF ZnO-Doped polystyrene nanocomposites: Structural, optical and defect analysis. Journal of Thermoplastic Composite Materials. 2024;0(0). doi:10.1177/08927057241291794

[3] Kacem, E., Althobaiti, H.A., Al-Ejji, M., Bader, N., Abed, A., Rajeh, A. Structural, optical, and thermal studies of Poly(vinylidene fluoride-co-hexafluoropropylene) and Polyvinylpyrrolidone composite doped Ag/ZnO mixed nanoparticles for flexible optoelectronic devices. Opt. Mater. 146 (2023) 114560.

https://doi.org/10.1016/j.optmat.2023.114560

[4] Ramazanov, M. A., &Rahimli, A. M. (2019). The Study of the Morphology and Dielectric Properties of PVC + TiO_2-Based Nanocomposites. Integrated Ferroelectrics, 201(1), 178–182. https://doi.org/10.1080/10584587.2019.1668701

[5] Mahammadali A Ramazanov, Almara M Rahimli. The Effect of the Temperature-Time Mode of Crystallization on the Photoluminescence and Dielectric Properties of PVC/TiO2 Nanocomposites. Integrated Ferroelectrics, 2020, 212(1), 61-67. https://doi.org/10.1080/10584587.2020.1819035

[6] Ramazanov, M. A., Rahimli, A. M., &Hajiyeva, F. V. (2020). The influence of titanium

dioxide (TiO_2) nanoparticles on the structure, optical and dielectric properties of polyvinyl chloride (PVC). Modern Physics Letters B, 34(28). https://doi.org/10.1142/S0217984920503108

[7] Bendaoued, A., Messaoud, M., Harzallah, O., Bistac, S., Salhi, R. "Nano-TiO_2 effect on thermal, rheological and structural properties of thermoplastic polypropylene nanocomposites," Journal of Materials Research and Technology, 2022, 17. 2313-2325. https://doi.org/10.1016/j.jmrt.2022.01.114.

[8] Alsulami, Q.A., Rajeh, A. "Structural, thermal, optical characterizations of polyaniline/polymethyl methacrylate composite doped by titanium dioxide nanoparticles as an application in optoelectronic devices". Optical Materials, 2022, 123, 111820 https://doi.org/10.1016/j.optmat.2021.111820.

[9] Esthappan, S.K., Kuttappan, S.K., Joseph, R. "Thermal and mechanical properties of polypropylene/titanium dioxide nanocomposite fibers," Materials & Design, 2012, 37, 537-542. https://doi.org/10.1016/j.matdes.2012.01.038.

[10] Dimitris N. Bikiaris, George Z. Papageorgiou, EleniPavlidou, NikolaosVouroutzis, ParaskevasPalatzoglou, George P. Karayannidis. "Preparation by melt mixing and characterization of isotactic polypropylene/SiO_2nanocomposites containing untreated and surface-treated nanoparticles," Journal of Applied Polymer Science, https://doi.org/10.1002/app.22849

[11] HassanzadehTabrizi, S. A. (2022). Synthesis, characterization, and magnetic properties of $NiFe_2O_4$ nanoparticles. Journal of Particle Science and Technology, 8, 79-85.

[12] Nath, D., Singh, F., & Yes, R. (2019). X-ray diffraction analysis by Williamson-Hall, Halder-Wagner, and size-strain plot methods of CdSe nanoparticles - A comparative study. Materials Chemistry and Physics, 239, 122021.

[13] Pandiyarajan, T., &Karthikeyan, B. (2012). Cr doping induced structural, phonon, and excitonic properties of ZnO nanoparticles. J. Nanopart. Res., 14, 647-656. https://doi.org/10.1007/s11051-011-0647-x

[14] Gareso, P., Heryanto, H., Sampebatu, E., Sampe, N., Palentek, V., Taba, P., Juarlin, Eko, &Aryanto, D. (2021). Synthesis and material characterization of TiO_2 nanoparticles doped with iron (Fe). Journal of Physics: Conference Series, 1763, 012059. https://doi.org/10.1088/1742-6596/1763/1/012059.

[15] Huseynova, A.S., Rzayev, R.M., Hajiyeva, F.V. Influence of electrothermopolarization process on the structure and properties of nanocomposites based on high-density polyethylene and HfO2 nanoparticles. J. Korean Physical Society. https://doi.org/10.1007/s40042-024-01094-8

[16] Saladino, M.L., Motaung, T.E., Luyt, A.S. et al. The effect of silica nanoparticles on the morphology, mechanical properties and thermal degradation kinetics of PMMA. Polymerdegradationandstability, 2012. 97 (3), 452-459. https://doi.org/10.1016/j.polymdegradstab.2011.11.006

[17] Bikiaris, D. N., &Matzinos, P. (2011). Can nanoparticles really enhance thermal stability of polymers? Part II: An overview on thermal decomposition of polycondensation polymers. ThermochimicaActa, 523(1), 25-45. https://doi.org/10.1016/j.tca.2011.06.012

[18] Klaudia, K., Kinga, P. Thermal Decomposition of Polymer Nanocomposites with Functionalized Nanoparticles. PolymerCompositeswithFunctionalizedNanoparticles, 2019, p. 405–435. doi:10.1016/b978-0-12-814064-2.00013-5.

[19] Ramazanov M.A.; Huseynova A.S.; Eyubova N.A.; Abasov S.A. J. of Optoelectronics and Advandced materials, vol 4, № 12, December, 2010,

[20] Alhussain, H., Alghamdi, A.M., Elamin, N.Y., Rajeh, A. Recent Progress in Enhanced Optical, Mechanical, Thermal Properties, and Antibacterial Activity of the Chitosan/Polyvinylalcohol/Co3O4 Nanocomposites for Optoelectronics and Biological Applications. Environ. Polym. Degrad. (2024) 32(8):1-14. DOI:10.1007/s10924-024-03191-y .

[21] Alqarni, L.S., Alghamdi, A.M., Elamin, N.Y., Rajeh, A. Enhancing the optical, electrical, dielectric properties and antimicrobial activity of chitosan/gelatin incorporated with Co-doped ZnO nanoparticles: Nanocomposites for use in energy storage and food packaging. Mol. Struct. 1297(1) (2024) 137011. https://doi.org/10.1016/j.molstruc.2023.137011

[22] Yabagi, J., Mohammed Kimpa, I., Muhammad, M., Rashid, S., Embong, Z., &Agam, M. (2018). The effect of gamma irradiation on chemical, morphology and optical properties of polystyrene nanosphere at various exposure time. IOP Conference Series: Materials Science and Engineering, 298, 012004. https://doi.org/10.1088/1757-899X/298/1/012004

[23] Castrejón-Sánchez, V. H., Camps, E., & Camacho-López, M. (2014). Quantification of phase content in TiO_2 thin films by Raman spectroscopy. Superficies y Vacío, 27(3), Ciudad de México.

[24] Alsalmah, H.A., Rajeh, A., Nur, O. Optical, conductivity, dielectric, and magnetic properties of polymer nanocomposite based on PAM/cs matrix and ZnFe2O4 NPs for use in magneto-electronic and energy storage capacitor devices. Ceram. Int. 50(7B) (2024) 12167–12174. https://doi.org/10.1016/j.ceramint.2024.01.120